PERGAMON

International Journal of Heat and Mass Transfer 44 (2001) 429–442

International Journal of
HEAT and MASS
TRANSFER

www.elsevier.com/locate/ijhmt

Temperature profile in countercurrent/cocurrent spray towers

N. Makkinejad

Lurgi Lentjes Bischoff GmbH, Bonsiepen 13, D-45136 Essen, Germany

Received 16 September 1999; received in revised form 16 February 2000

Abstract

The classical theory of the cooling tower does not include a suitable mathematical solution for a direct and quick calculation of gas/liquid temperature profiles. This forces in most of practical cases, for example in case of industrial spray absorbers, to simplify the problem and to assume a complete cooling of exit gases down to the adiabatic saturation temperature of the incoming gases. In the present paper, a new method is described to develop an acceptable mathematical solution for cooling towers, taking into account the main influencing parameters, especially the liquid to gas ratio (L/G) and the actual liquid and gas interface. Calculations with the new solution show, that the exit gas temperature is strongly influenced by the liquid inlet temperature. In case of closed loop and counter current systems, this liquid inlet temperature is more or less close to the adiabatic saturation temperature of the incoming gases. In these cases, the exit gas temperature is only slightly higher than the currently assumed adiabatic saturation temperature of the inlet gases. This is completely different to the open loop systems, where the liquid inlet temperature is not influenced by the incoming gases at all. In these cases, the gas outlet temperature is mostly far from the adiabatic saturation temperature of the inlet gases, so that the current assumption can initiate great errors. © 2000 Elsevier Science Ltd. All rights reserved.

Keywords: Cooling towers; Evaporation; Modeling

1. Introduction

In a lot of different technical processes, hot gases are quenched in spray towers with water or some other solutions, to cool them down directly. Spray towers are also often used, to scrub technical gases, which are automatically cooled down in parallel. In some other cases, spray towers are used to cool hot water by aeration and by evaporation.

The mathematical handling of these processes leads to a relatively simple system of simultaneous differential equations (DEqs.), without being solved analytically up to now. This again is caused by dependency, between the saturation humidity and temperature of the gases and the related gas properties.

The importance of technical cooling and absorption processes has nevertheless forced to develop useful approximate solutions. To reach that, two important ways have been established in the classical theory of cooling tower. The first one simplifies the problem and assumes constant saturation properties at the gas/liquid interface throughout the tower, so that the explicit integration of the related DEqs. becomes possible. This simplification can

---

E-mail address: makkinejad@lbischoff.de (N. Makkinejad).

PII: S0017-9310(00)00088-0

Nomenclature

A	total interface area in tower (m^2)
A_I	lateral surface of one droplet (m^2)
a	specific interface area per unit of tower height (m^2/m)
c_{pG}	heat capacity of dry gas between 0°C and t ($kJ/kg_{dry}/K$)
c_{pD}	heat capacity of vapor between 0°C and t (kJ/kg/K)
c_L	heat capacity of liquid (here water) (kJ/kg/K)
c_W	drag coefficient
D	diameter (m)
dH	height of the tower segment (m)
$\dot{G}$	dry gas flow rate (kmol/s)
$g = 9.81$	acceleration of gravity (m/s^2)
H	tower vertical coordinate from bottom to the top (m)
H_K	tower height (m)
$\dot{L}$	liquid flow rate (here water) (kmol/s)
$\dot{m}$	liquid as well as vapor flow rate (kg/s)
$\dot{m}_{Abs}$	total absorption flow rate of the tower (kg/s)
M	molecular weight (kg/kmol)
m, n	counting variables
$\dot{n}$	specific molecular flow rate ($kmol/m^2/s$)
p	pressure (bar)
$\dot{Q}$	heat flow rate (kJ/s)
q_{Abs}	absorption heat (kJ/kg)
r_0	evaporation heat of water at 0°C (kJ/kg)
t	gas temperature (°C)
V	volume (m^3)
V_1	volume of one droplet (m^3)
w	velocity (m/s)
w_F	mean falling down velocity of uniform droplets (m/s)
x	absolute gas humidity (kg/kg_{dry})
x_P	local absolute gas humidity at interface (kg/kg_{dry})
y	vertical tower coordinate from top to bottom (m)
y_{Cl}	chloride content of the liquid (here water) ($kmol/m^3$)
z	time (s)

Greek symbols

α	heat transfer coefficient ($kW/m^2/K$)
β	mass transfer coefficient ($kmol/m^2/s$)
ρ	density of pure materials (water, gas) (kg/m^3)
ρ^*	density of mixtures (kg/m^3)
ϑ	liquid temperature (here water) (°C)

Indices

Ab	removed (water or heat)
B	bottom
D	vapor
F	falling
G	gas (dry gas)
K	head (top of the tower)
L	liquid
P	phase interface
PB	interface at tower bottom
PK	interface at tower top
rel	relative
R	back flow
S	sauter (diameter)
s	saturation (pressure and temperature) (also boiling pressure and temperature)
T	tower
Tr	droplet
tr	dry
Z	make up; supply

only be tolerated for very small changes of the liquid and gas temperature, like those in a small tower segment. Therefore, the integration has to be carried out segment by segment and put together for a real big tower [1, pp. 35–51]. A complicated procedure, which is not suitable for fast parameter variations and numerical calculations, is required for design optimization.

The second way linearizes the gas saturation enthalpy (operating line) over the liquid enthalpy, i.e. the liquid temperature, and integrates the DEq. belonging to it either graphical or numerical [1, p. 63, 2, Section 12, p. 12]. This method, named after Sherwood, is mostly used to design cooling towers. However, it is not suitable for calculation of temperature profiles in the tower because of its inconvenience.

A further improvement of this method in Europe has led to the introduction of a so-called "evaporation number" (known as Merkel number), which helps to save calculation time but still needs manual iterations [3–5].

In this paper, a new way is described to develop a better approximate solution without the above mentioned disadvantages. The analytical integration of the resulting DEq. is impossible because of the presence of some disturbing parameters. The new calculation method generalizes the Sherwood idea and linearizes all the disturbing parameters within their boundary values. At the boundaries themselves, there is no difference between the real and linearized distribution. Marginal differences can only appear far from the boundaries, but they are still small compared with the actual values, and can be tolerated in most cases. The linearization is only used to win the approximate analytical solution of the problem. After that, there is no need to replace the real dependencies by linear distributions. This improves the correspondence of the approximate solution with the reality.

Due to the arbitrariness of this step, the linearization does not need necessarily to be executed over the local coordinate (tower height). It can be realized over any other belonging and suitable system parameter. The method can also be used in other similar cases of mathematical physics.

2. Gas/liquid contact in open loops

In the following, a countercurrent spray tower is considered and primarily dealt with in details. Continuous gas and liquid flows with constant temperature and composition at the tower inlet are assumed. The inlet temperatures are absolutely independent from the outlet temperatures (open loop). Further, a steady state is assumed, e.g. any existing non stationary start-up period is finished so that the temperature profile over the tower does not change with the time any more.

Inside the tower, a complete equalized gas and droplet distribution over the tower section is assumed. It is also assumed that the liquid stream is fed totally to the spray nozzles in a single bank located at the top of the tower, falling uniformly through the total tower height.

The developed solution includes a simultaneous exothermic absorption of a gas component, to make it also accessible for absorption towers. The influence of chloride ions on saturation properties is also taken into account because of its importance in some real industrial cases.

The mechanism of the absorption in the tower is very similar to that of gas humidification. This makes the exact handling of the present main problem very difficult. The absorption rate is not the most important influencing parameter for calculation of the temperature profile. Therefore, it seems acceptable to simplify the problem by assuming a constant specific absorption rate over the tower height, without loosing too much accuracy. This linearization can be realized over the absolute gas humidity x as well and leads, as it will be shown later, to a more realistic exponential shape of the absorption rate over the tower height.

The procedure for cocurrent spray towers is similar, but not described here. The related solutions are nevertheless included in this paper. In all these solutions, the liquid falls from the top to the bottom of the tower.

2.1. Mass and energy balance for the tower segment

Balancing the input/output mass and heat streams of the tower segment (Fig. 1) leads with the assumed uniform specific absorption rate to the following DEqs.:

$$\mathrm{d}\dot{L} = -\frac{M_\mathrm{G}}{M_\mathrm{L}} \cdot \dot{G} \cdot \mathrm{d}x \tag{1}$$

$$c_\mathrm{pG} \cdot \mathrm{d}t + c_\mathrm{pD} \cdot \mathrm{d}(x \cdot t) + r_0 \cdot \mathrm{d}x + \frac{M_\mathrm{L} \cdot c_\mathrm{L}}{\dot{G} \cdot M_\mathrm{G}} \cdot \mathrm{d}(\vartheta \cdot \dot{L}) = \pm \frac{\dot{m}_\mathrm{Abs} \cdot q_\mathrm{Abs}}{\dot{G} \cdot M_\mathrm{G}(x_\mathrm{K} - x_\mathrm{B})} \cdot \mathrm{d}x \tag{2}$$

The integration of these DEqs. with regard to the related boundary conditions leads to the solutions:

$$\dot{L} = \dot{L}_\mathrm{B} \pm \frac{M_\mathrm{G}}{M_\mathrm{L}} \cdot \dot{G}(x - x_\mathrm{B}) = \dot{L}_\mathrm{K} \pm \frac{M_\mathrm{G}}{M_\mathrm{L}} \cdot \dot{G}(x - x_\mathrm{K}) \tag{3}$$

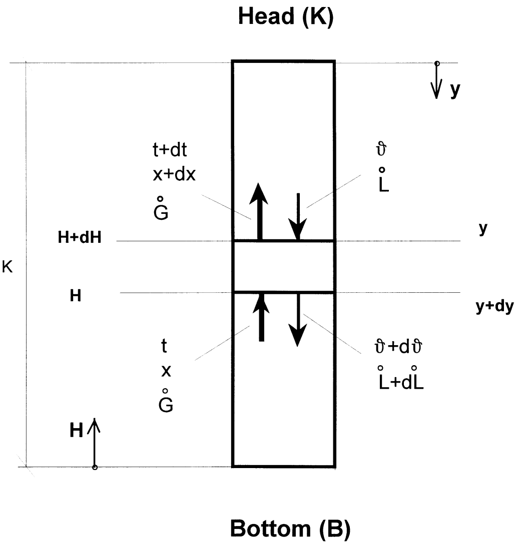

Fig. 1. Gas and liquid streams through the tower segment.

$$\vartheta = \frac{\dot{L}_\mathrm{K}}{\dot{L}} \left\{ \vartheta_\mathrm{K} \pm \frac{\dot{G} \cdot M_\mathrm{G}}{\dot{L}_\mathrm{K} \cdot M_\mathrm{L}} \cdot \frac{1}{c_\mathrm{L}} \big[c_\mathrm{pG}(t - t_\mathrm{K}) + c_\mathrm{pD}(x \cdot t - x_\mathrm{K} \cdot t_\mathrm{K}) + r_0(x - x_\mathrm{K}) \big] + \frac{1}{c_\mathrm{L}} \cdot \frac{\dot{m}_\mathrm{Abs} \cdot q_\mathrm{Abs}}{\dot{L}_\mathrm{K} \cdot M_\mathrm{L}} \cdot \frac{x_\mathrm{K} - x}{x_\mathrm{K} - x_\mathrm{B}} \right\} \qquad (4)$$

In above solutions "+" is valid for countercurrent and "–" for cocurrent spray towers.

2.2. Mass and energy balance for the gas stream alone

Immediately at the interface (Fig. 2), there is a lively mass and energy exchange between gas and liquid. The transferred mass and energy amounts between the liquid droplets and the gas phase in the tower segment (caused by evaporation, absorption and heat convection) are equal to the mass and energy changes of the gas stream flowing through the segment. This leads finally with respect to the Lewis law, to the following DEqs.:

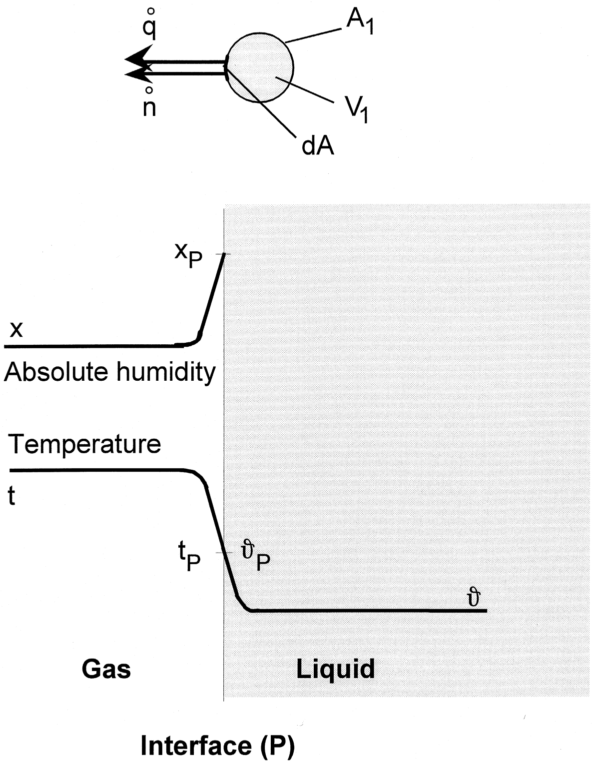

Fig. 2. Distribution of absolute humidity and temperature at interface.

$$\frac{\mathrm{d}x}{x_\mathrm{P} - x} \pm \frac{\beta \cdot M_\mathrm{L} \cdot a_\mathrm{T}}{\dot{G} \cdot M_\mathrm{G}} \cdot \mathrm{d}y = 0 \qquad (5)$$

$$\frac{\mathrm{d}t}{\mathrm{d}x} - \frac{c_\mathrm{pG} + (x_\mathrm{P} - x) \cdot c_\mathrm{pD}}{(c_\mathrm{pG} + x \cdot c_\mathrm{pD}) \cdot (x_\mathrm{P} - x)} (\vartheta_\mathrm{P} - t) = 0 \qquad (6)$$

Here again, "+" is valid for countercurrent and "–" for cocurrent spray towers.

The above DEqs. include beside the mass transfer coefficient β, the absolute humidity x_P and the temperature ϑ_P at the interface as well as the specific interfacial area a_T of the tower. So the integration can only be initiated after analysing and defining these parameters.

The mass transfer coefficient β can be estimated as usual via the heat transfer coefficient α [1, p. 57]

$$\beta = \frac{\alpha}{M_\mathrm{L} \cdot c_\mathrm{pG}} \qquad (7)$$

(This mass transfer coefficient is known after Lewis as evaporation coefficient σ and given in kg/m^2/s.)

The heat transfer coefficient α is calculated on the basis of the thermodynamic similarity laws (for spheres in gas streams) as a function of Nusselt number.

The calculation of the interfacial area in the tower is a little more complicated because the sprayed liquid consists of a multitude of droplets with different shapes and sizes. Their permanent mutual influence by accidental collision, coalescence and break up, makes an exact mathematical recording impossible. However, the experience shows that any spray tower type has his own characteristic specific interfacial area, which can be defined by evaluation of operating data of that tower. This factum allows the current simplification, to replace all the droplets by spheres of different sizes and to replace this inhomogeneous ensemble by an equivalent uniform sized drop population having the same total volume and exchange surface.

The so-defined diameter of the equalized spheres $D_\mathrm{S} = \Sigma d^3 / \Sigma d^2$ is called after Sauter and can be estimated as the 63.2% passage diameter, if the diameter distribution is plotted in a Rosin–Rammler–Sperling diagram [6].

The diameter distribution of droplets generated by individual spray nozzles can be measured easily under laboratory conditions. Therefore, the Sauter diameter of the droplets produced by the installed nozzles is normally known for different flow rates respectively pressures.

Coalescence of small droplets to new bigger droplets in the spray tower leads to an increase in this Sauter diameter. The tower wall has the same result, where a part of sprayed liquid is collected and a single flowing liquid film is built. In contrast to this continuous evaporation as well as break up of bigger droplets into several smaller droplets caused by collisions or gas influence reduce the Sauter diameter.

The direct measurement of droplet sizes in the spray tower under operating conditions is difficult and accompanied by uncertainties. This means that in practical cases the Sauter diameter has to be calculated based on interpretation of easy measurable operating parameters, demonstrated by an example at the end of this paper. For big industrial spray towers, the Sauter diameter of the individual nozzles can be used as a first approach because the wall effect is not so important. (The specific wall surface area per unit volume of the tower is proportional to $1/D_T$ and decreases with increasing tower diameter D_T.)

The time-dependent motion of the equalized droplets, under the action of gravity and with respect to the drag force caused by the different gas and droplet velocities, can be formulated based on the laws of mechanics. The residence time of each droplet in the contact zone between top and bottom of the tower can be calculated by setting $y = H_K$ and $z = z_F$ in the motion equation $y = f(z)$. This leads to the following relation assuming constant gas velocity and drag coefficient, which has to be solved by iteration:

$$z_F = \frac{1}{\sqrt{g/K} \mp w_G}\left\{H_K - \frac{1}{K}\cdot\ln\left[\frac{w_K \pm w_G + \sqrt{g/K}}{2\cdot\sqrt{g/K}} - \frac{w_K \pm w_G - \sqrt{g/K}}{2\cdot\sqrt{g/K}}\cdot\exp\left(-2\cdot K\cdot\sqrt{g/K}\cdot z_F\right)\right]\right\} \tag{8}$$

In this equation, the top "+/−" sign is valid for countercurrent and the lower sign for cocurrent spray towers. The abbreviation K is given by:

$$K = \frac{6}{8}\cdot\frac{c_W}{D_S}\cdot\frac{\rho_G^*}{\rho_L^* - \rho_G^*} \tag{9}$$

The mean droplet velocity, which may be used for the calculation of the drag coefficient c_W, can either be estimated as $w_F = H_K/z_F$ or as $w_F = (w_K + w_B)/2$.

Finally, the total interface area in the tower can be estimated as:

$$A = 6\cdot\frac{M_L\cdot\dot{L}_K}{\rho_L\cdot D_S}\cdot z_F \tag{10}$$

The falling velocity of the liquid droplets in the tower is not constant of course, so that the distribution of the interface area over the tower height is also not homogenous. Nevertheless, a homogenous distribution and a constant specific interfacial area over the tower height is assumed in the following as an acceptable simplification.

$$a_T = \frac{A}{H_K} = 6\cdot\frac{M_L\cdot\dot{L}_K}{D_S\cdot\rho_L}\cdot\frac{z_F}{H_K} \tag{11}$$

For calculation of the local absolute humidity x_P and temperature $t_P = \vartheta_P$ at the interface, following relation will be used representing primarily the dependency of the boiling pressure and boiling temperature of water including some chloride ions [7, pp. 40–42]. It also includes the dependency of vapor pressure of water, saturation humidity and total pressure, assuming that the gas at the interface is already saturated. This assumption is justified by the fact that here a kind of thermodynamic equilibrium exists, so that the local absolute humidity x_P corresponds exactly to the vapor pressure p_S. In other words, the interface temperature (wet bulb temperature) $t_P = \vartheta_P$ is identical with the saturation temperature t_S.

$$\vartheta_P = \frac{5154.311}{13.8259 - \frac{M_L}{\rho_L}\cdot y_{Cl} - \ln\left(\frac{p}{\mathrm{bar}}\cdot\frac{M_G\cdot x_P}{M_L + M_G\cdot x_P}\right)} - 273.15 \tag{12}$$

This relation is suitable in the range of 20–100°C, because its constants are determined based on the known pressures at these temperatures.

In Eqs. (12) and (6), ϑ_P can be replaced by ϑ, because the liquid side heat transfer coefficient α_L for convective heat exchange between water and its interface is much greater than the gas side heat transfer coefficient α [1, p. 23/37]. This is done in the following in accordance with the common praxis.

Owing to the complicated relationship between x_P and $t_P = \vartheta_P$ as shown in Eq. (12), the analytical integration of the DEqs. (5) and (6) is not possible. However, as already mentioned, there is a possibility to develop suitable approximate solutions with relative small and acceptable deviations. To achieve this, the variables x_P and ϑ_P, i.e. ϑ, should be linearized within their boundary values at the top and bottom of the tower. For the liquid temperature ϑ, the tower height H, as also the absolute humidity x can act as the obvious independent variable over which the linearization takes place. The use of x is preferred in the following because it creates an exponential height dependency, which covers the real conditions much better.

$$\vartheta = \vartheta_B + \frac{x - x_B}{x_K - x_B}(\vartheta_K - \vartheta_B) \tag{13}$$

For the absolute humidity x_P at the interface, the interface temperature ϑ_P (i.e. liquid temperature ϑ, as $\alpha_L \gg \alpha$ has been assumed) is the determining natural independent variable. This leads to the linear relation:

$$x_P = x_{PB} + \frac{\vartheta - \vartheta_B}{\vartheta_K - \vartheta_B} \cdot (x_{PK} - x_{PB}) \tag{14a}$$

This equation, modified with respect to Eq. (13), leads again to a relation, in which x becomes the obvious independent variable:

$$x_P = x_{PB} + \frac{x - x_B}{x_K - x_B} \cdot (x_{PK} - x_{PB}) \tag{14b}$$

The above linearization is also physically admissible because the saturation curve of water vapor in the related range has a slight curvature only.

It should be noted here again that the linear relations (13) and (14b) properly have the only aim, to allow an acceptable approximate integration of the DEqs. (5) and (6), without replacing the real dependencies of the liquid temperature and the local absolute humidity at the interface.

It should further be noted that the classical Sherwood method uses a similar linearization as well to define the "operating line". This is done without developing an analytical solution. The approximated "operating line" replaces the real dependencies of the related parameters.

Substituting Eq. (14b) into DEq. (5), makes it simply integrable. The solution with respect to the boundary conditions is as follows:

$$x = \frac{\xi}{1-\eta} - \left(\frac{\xi}{1-\eta} - x_B\right) \cdot \exp\left[-K_0(1-\eta) \cdot H\right] \tag{15}$$

For cocurrent spray towers "H" has to be replaced by "y" and "x_B" by "x_K". The used abbreviations are defined as:

$$\eta = \frac{x_{PK} - x_{PB}}{x_K - x_B} \tag{16}$$

$$\xi = x_{PB} - \eta \cdot x_B \quad \text{(for countercurrent towers)} \tag{17a}$$

$$\xi = x_{PK} - \eta \cdot x_K \quad \text{(for cocurrent towers)} \tag{17b}$$

$$K_0 = a_T \cdot \frac{\beta \cdot M_L}{\dot{G} \cdot M_G} \tag{18}$$

With Eqs. (13) and (14b), the DEq. (6) takes the simple form:

$$\frac{dt}{dx} + p(x) \cdot t + q(x) = 0 \tag{19}$$

Now this DEq. can be integrated [8, pp. 378, 288 and 299; 9, pp. 170 and 91]. The solution for different cases, fitted to the corresponding boundary conditions is given below:

(i) In case of $\xi = 0$ and $\eta = 1$, i.e. for $\xi - (1-\eta) \cdot x = 0$:

$$t = \vartheta \tag{20a}$$

(ii) In case of $\xi - (1-\eta) \cdot x \neq 0$:

$$t = \tau + x \cdot \varsigma + (t_B - \tau - x_B \cdot \varsigma) \cdot \frac{Z_1(x)}{Z_1(x_B)} + Z_1(x)\left[Z_2(x_B) - Z_2(x)\right] \cdot \varsigma \tag{20b}$$

For cocurrent towers, index B (bottom) should be replaced by K (head). The new abbreviations mean:

$$\varsigma = \frac{\vartheta_K - \vartheta_B}{x_K - x_B} \tag{21}$$

$$\tau = \vartheta_B - x_B \cdot \varsigma \quad \text{(for countercurrent tower)} \tag{22a}$$

$$\tau = \vartheta_K - x_K \cdot \varsigma \quad \text{(for cocurrent tower)} \tag{22b}$$

The particular solution $Z_1(x)$ for both, countercurrent and cocurrent spray towers is defined as follows:

(i) In case of $1 - \eta \neq 0$:

$$Z_1(x) = \left[\varphi \cdot \text{abs}(1-\eta)\right]^{-1/2} \cdot \frac{\varphi}{1 + x \cdot \varphi}\left[\frac{\varphi}{1 + x \cdot \varphi} \cdot \text{abs}\left(\frac{\xi}{1-\eta} - x\right)\right]^{1/\delta} \tag{23a}$$

(ii) In case of $1 - \eta = 0$:

$$Z_1(x) = (1 + x \cdot \varphi)^{-\dfrac{1 + \xi \cdot \varphi}{\xi \cdot \varphi}} \tag{23b}$$

The new abbreviations mean:

$$\varphi = \frac{c_{pD}}{c_{pG}} \tag{24}$$

$$\delta = \xi \cdot \varphi + 1 - \eta \tag{25}$$

To define the second function $Z_2(x)$ in Eq. (20b), following additional abbreviations are introduced:

$$\gamma = \frac{1}{\text{abs}(\delta)} \tag{26}$$

$$\psi = \text{sign}(1-\eta) \tag{27}$$

$$\mu = (1 + x \cdot \varphi) \cdot \text{abs}\left(\frac{1-\eta}{\delta}\right) \tag{28}$$

For $Z_2(x)$ itself, the following different cases will occur:

(i) In case of $1-\eta \neq 0$:

There exist different solutions depending on the behavior of μ:

1. $\mu < 1$:

$$Z_2(x) = \sqrt{\varphi \cdot \mathrm{abs}(1-\eta)} \cdot \left(\frac{1+x\cdot\varphi}{\varphi}\right)^2 \cdot \mu^{1/\delta} \cdot \left[\frac{1}{2\pm\gamma} + \sum_{m=1}^{\infty} \frac{\psi^m}{2\pm\gamma+m} \cdot \prod_{n=0}^{m-1}\left(\frac{\gamma\pm n}{n+1}\cdot\mu\right)\right] \tag{29}$$

In this solution, "+" is valid for $\delta > 0$ and "−" for $\delta < 0$. In the last case when γ is an integer, then the infinite series will become finite with a limited number of $\gamma + 1$ terms. In addition to that, the term $1/(2-\gamma+\mathrm{m})$ for $\mathrm{m} \geq 0$ must be replaced by:

$$\frac{x\cdot\varphi}{1+x\cdot\varphi} \quad \text{for } \gamma = 1+\mathrm{m} \tag{30a}$$

or by

$$\ln(1+x\cdot\varphi) \quad \text{for } \gamma = 2+\mathrm{m} \tag{30b}$$

2. $\mu > 1$:

$$Z_2(x) = \sqrt{\varphi \cdot \mathrm{abs}(1-\eta)} \cdot \left(\frac{1+x\cdot\varphi}{\varphi}\right)^2 \cdot \mu^{1/\delta} \cdot \left[\frac{1}{2} + \gamma\cdot\frac{\psi}{\mu}\cdot\frac{x\cdot\varphi}{1+x\cdot\varphi} + \frac{\gamma}{\mu}\cdot\frac{\gamma\pm 1}{2\cdot\mu} \cdot \ln(1+x\cdot\varphi) + \sum_{m=3}^{\infty}\frac{\psi^m}{2-m} \cdot \prod_{n=0}^{m-1}\left(\frac{\gamma\pm n}{n+1}\cdot\frac{1}{\mu}\right)\right] \tag{31}$$

Here as well, "+" is valid for $\delta > 0$ and "−" for $\delta < 0$. Similar to case (1), for $\delta < 0$, the infinite series will become finite with only $\gamma + 1$ terms, if γ is an integer.

(ii) In case of $1-\eta = 0$:

$$Z_2(x) = \frac{\xi}{1+2\cdot\xi\cdot\varphi}(1+x\cdot\varphi)^{\frac{1+2\cdot\xi\cdot\varphi}{\xi\cdot\varphi}} \tag{32}$$

The "binomial series" in Eqs. (29) and (31) are mostly converging continuously except in some special cases. In such cases the solution fails because the addition of the series must be interrupted before convergence is achieved. If this happens, the calculated local absolute humidity at the tower outlet does not comply with the linearized one; a simple way to check the calculation.

The calculation has to be carried out by iteration. Estimated $\mathrm{w_G}$, $\mathrm{w_F}$, ρ^*_{G}, ϑ_{B} and x_{K} values help to calculate c_{W}, z_{F}, w_{B}, β and finally x_{K}, t_{K} and ϑ_{B}. So the initial estimation can be corrected for new calculations, until the required accuracy is reached.

Owing to the large volume of the work, the use of electronic calculators is absolutely necessary. A "quick basic" calculation program is available from the author.

3. Gas/liquid contact in closed loops

In most practical cases, the sprayed liquid is collected in a sump and recycled again via recycle pumps to the spray nozzles. That is the reason why the system is called a closed loop. In these cases, the liquid temperature ϑ_{K} at the top of the tower is influenced by the liquid temperature ϑ_{B} at the bottom of the tower. Once any start up period ends and the steady state is reached, the temperature ϑ_{K} can be calculated based on the energy balance of the sump. The results for different cases are given below:

(i) For gas cooling towers (Fig. 3)

$$\vartheta_{\mathrm{K}} = \frac{\dot{L}_{\mathrm{B}}\cdot\vartheta_{\mathrm{B}} + \left(\dot{L}_{\mathrm{K}} - \dot{L}_{\mathrm{B}} + \dot{L}_{\mathrm{Ab}}\right)\cdot\vartheta_{Z}}{\dot{L}_{\mathrm{K}} + \dot{L}_{\mathrm{Ab}}} \tag{33}$$

(ii) For liquid cooling towers (Fig. 4)

If in this case the removing heat flow $\dot{Q}_{\mathrm{Ab}}$ is known, then the solution is:

$$\vartheta_{\mathrm{K}} = \frac{\dot{L}_{\mathrm{B}}\cdot\vartheta_{\mathrm{B}} + \left(\dot{L}_{\mathrm{K}} - \dot{L}_{\mathrm{B}} + \dot{L}_{\mathrm{Ab}}\right)\cdot\vartheta_{Z} + \dfrac{\dot{Q}_{\mathrm{Ab}}}{M_{\mathrm{L}}\cdot c_{\mathrm{L}}}}{\dot{L}_{\mathrm{K}} + \dot{L}_{\mathrm{Ab}}} \tag{34a}$$

If instead of the removing heat flow the liquid back flow $\dot{L}_{\mathrm{R}}$ and its temperature ϑ_{R} are known, the solution will be:

$$\vartheta_{\mathrm{K}} = \frac{\dot{L}_{\mathrm{B}}\cdot\vartheta_{\mathrm{B}} + \left(\dot{L}_{\mathrm{K}} - \dot{L}_{\mathrm{B}} + \dot{L}_{\mathrm{Ab}}\right)\cdot\vartheta_{Z} + \dot{L}_{R}\cdot\vartheta_{R}}{\dot{L}_{\mathrm{K}} + \dot{L}_{\mathrm{Ab}} + \dot{L}_{R}} \tag{34b}$$

Similar to open loop systems, the calculation must also be done by iteration. The initially chosen temperature ϑ_{K} helps to calculate ϑ_{B} in accordance with the solutions for open loop systems. After that, a new ϑ_{K} can be calculated using Eqs. (33) or (34), acting as a better approach of the initial value. (A calculation program written in "quick basic" is also in this case available from the author.)

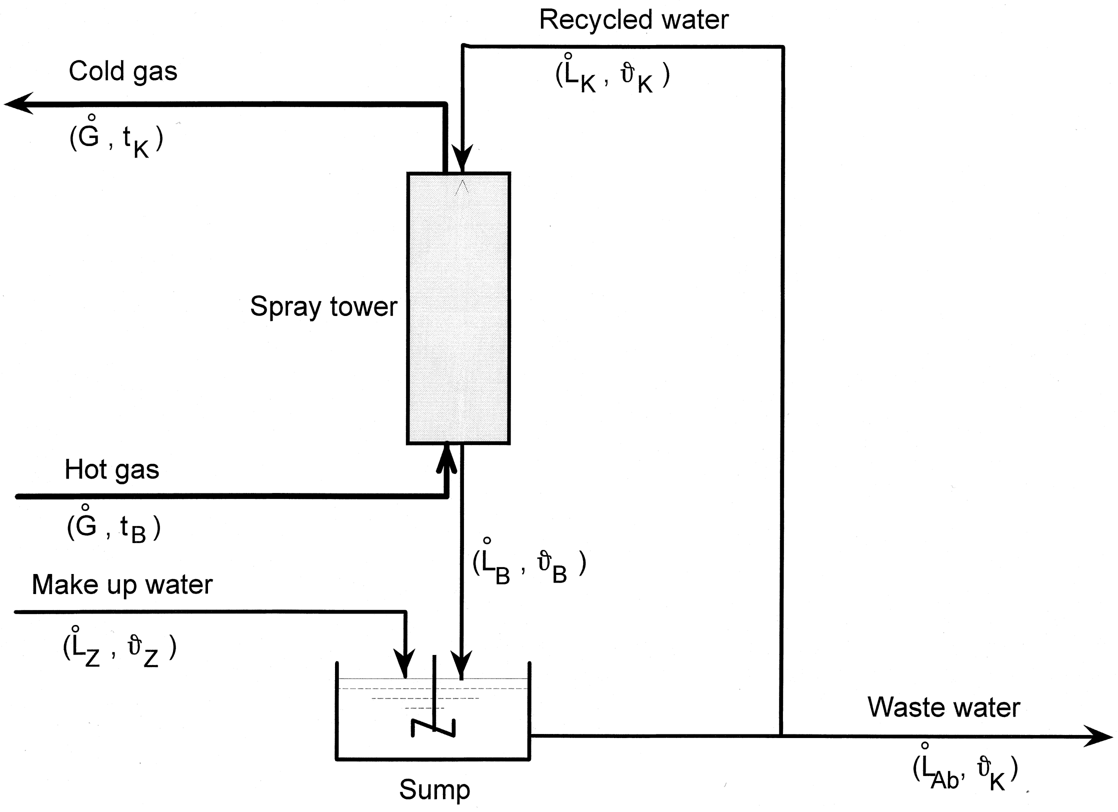

Fig. 3. Closed loop gas cooling tower.

4. Application of the theory

4.1. Open loop spray tower

To check and demonstrate the suitability of the developed solutions, some measured results of a pilot plant are used by way of comparison. The small pilot plant was built to test and demonstrate flue gas desulphurization with pure sea water (sea water scrubbing) behind a coal fired boiler. In this plant, fresh sea water (condenser cooling water) was brought in contact with flue gases in an open loop countercurrent spray tower, treated afterwards and returned to the sea. The operating and design parameters of the pilot plant are listed in Table 1.

To determine the actual characteristic droplet size of the tower, Fig. 5 was prepared based on the presented solutions, showing the calculated gas and liquid outlet temperatures versus assumed uniform droplet sizes. From this figure and based on the measured temperatures, the actual characteristic droplet diameter could be found equal to 2.12 mm. Obviously, the relative big wall effect causes here a significant increase in the Sauter diameter compared with that of the individual nozzle.

In Figs. 6 and 7, calculated temperature and

Table 1
Operating parameters and some test results of the pilot plant

Tower diameter	1.016 m
Tower height	6.3 m
Gas flow rate	0.084179 kmol/s
Gas inlet temperature	112.5°C
Inlet absolute humidity	0.0743 kg/kg_{dry}
Gas outlet temperature	48.7°C
Absorption rate	0.001558 kg/s (SO_2)
Liquid flow rate	0.4475 kmol/s
Liquid inlet temperature	33°C
Chloride content of liquid	0.5634 $kmol/m^3$
Number of operating spray banks	1
Number of nozzles per bank	1
Nozzle type	Hollow cone
Nozzle outlet velocity	6.0 m/s
Nozzle Sauter diameter	1.2 mm
Liquid outlet temperature	44.1°C

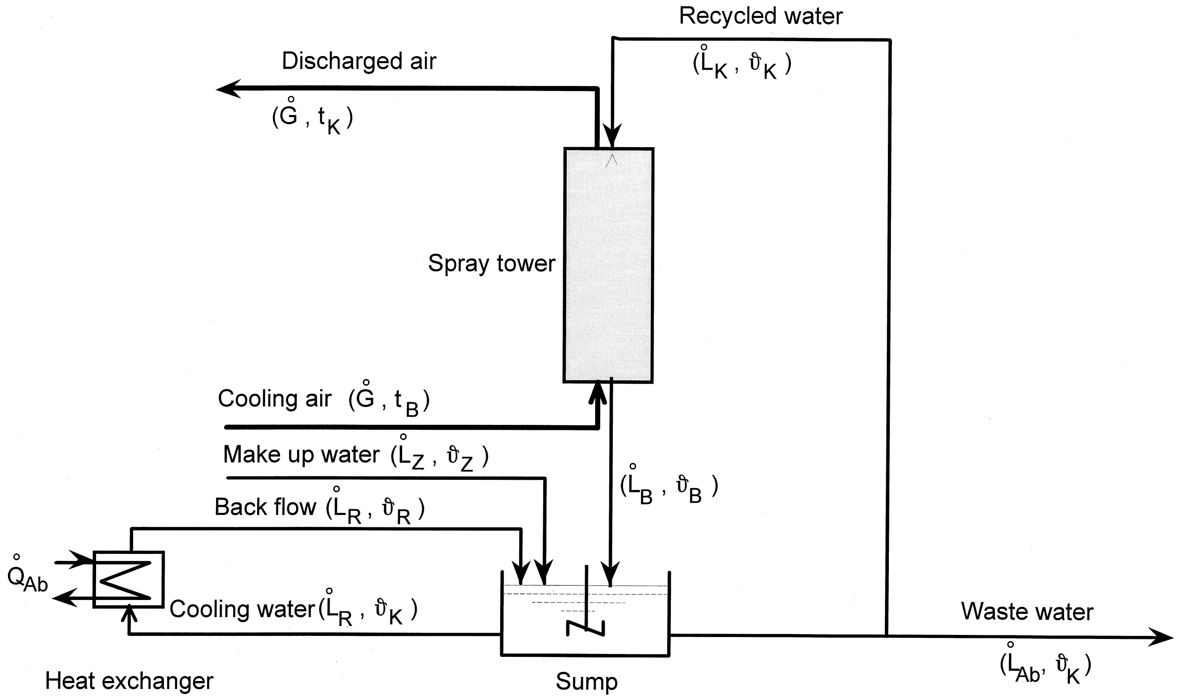

Fig. 4. Closed loop water cooling tower.

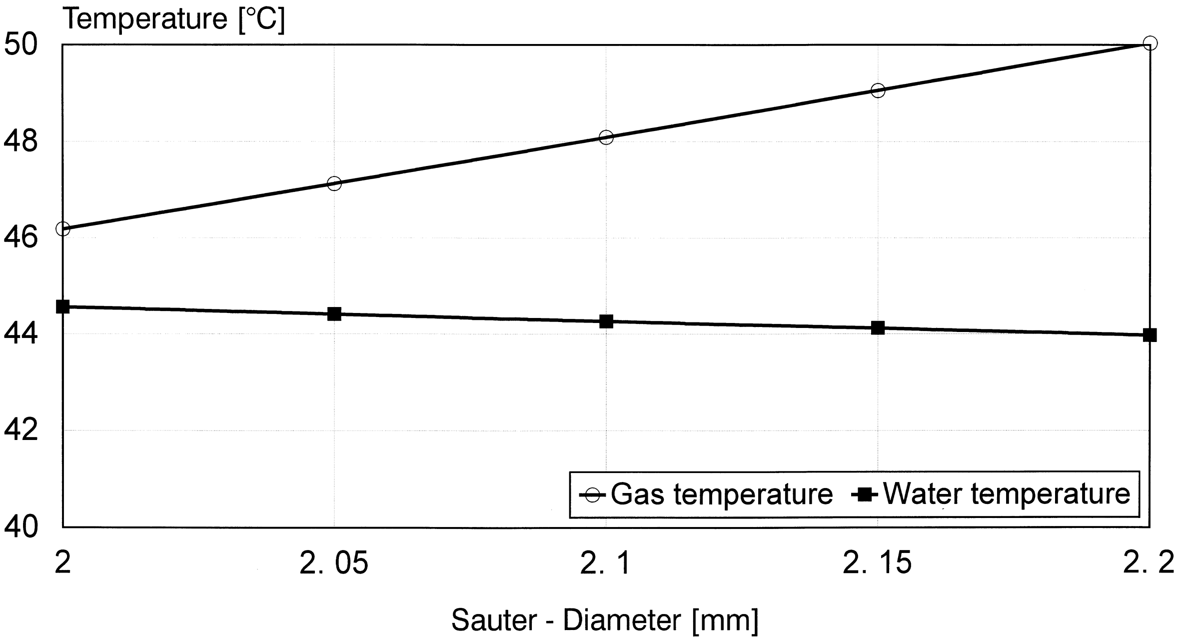

Fig. 5. Calculated outlet temperatures versus droplet size.

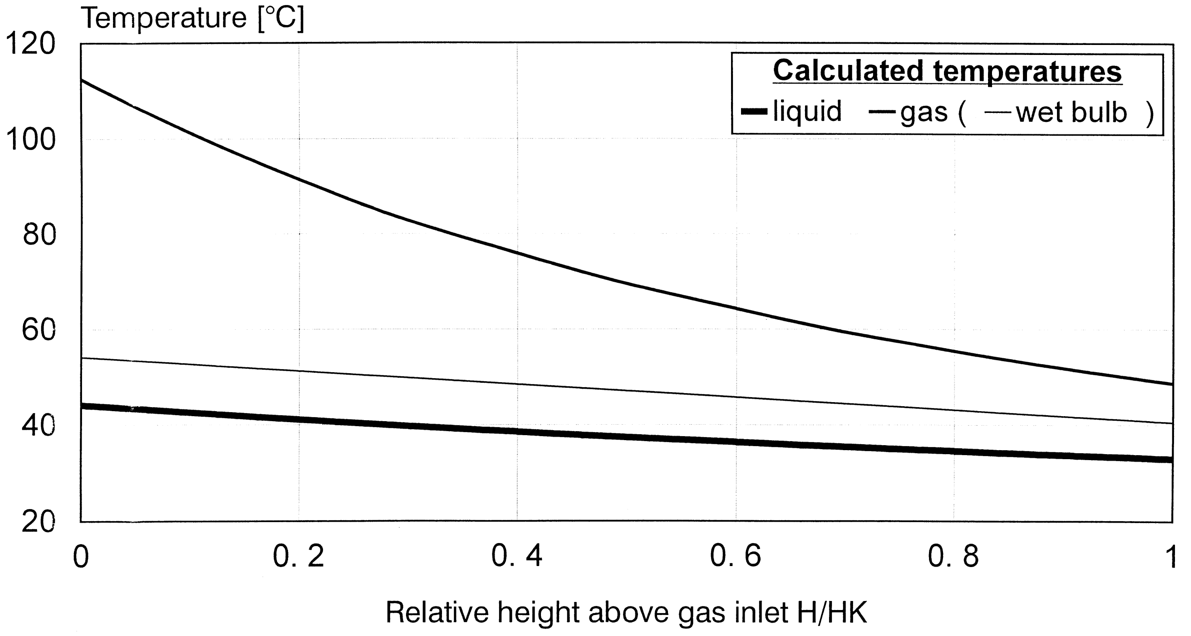

Fig. 6. Calculated temperatures for the pilot plant with open loop.

humidity profiles over the tower height are graphically shown, using the previously obtained actual Sauter diameter in the tower. The nearly perfect conformity of the linearized and non linearized values of the local interface absolute humidities at the tower boundaries shows that the series have had a good convergence. The maximum relative deviation of approximately 8.5% inside the tower allows the conclusion that the used linearization can be marked as acceptable.

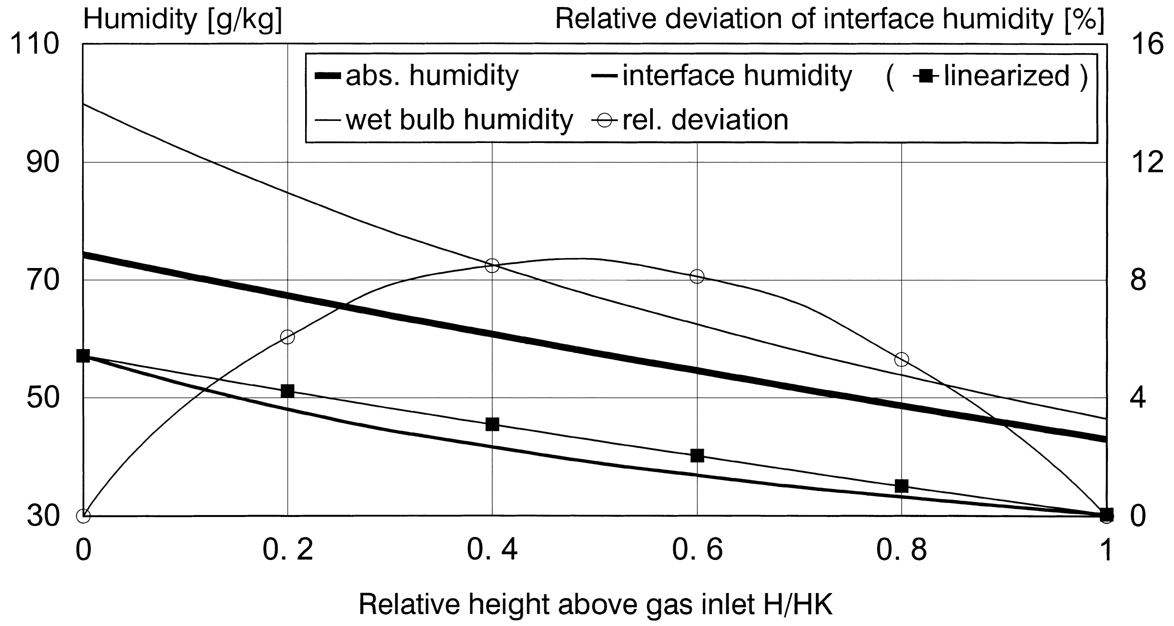

Fig. 7. Calculated humidities for the pilot plant with open loop.

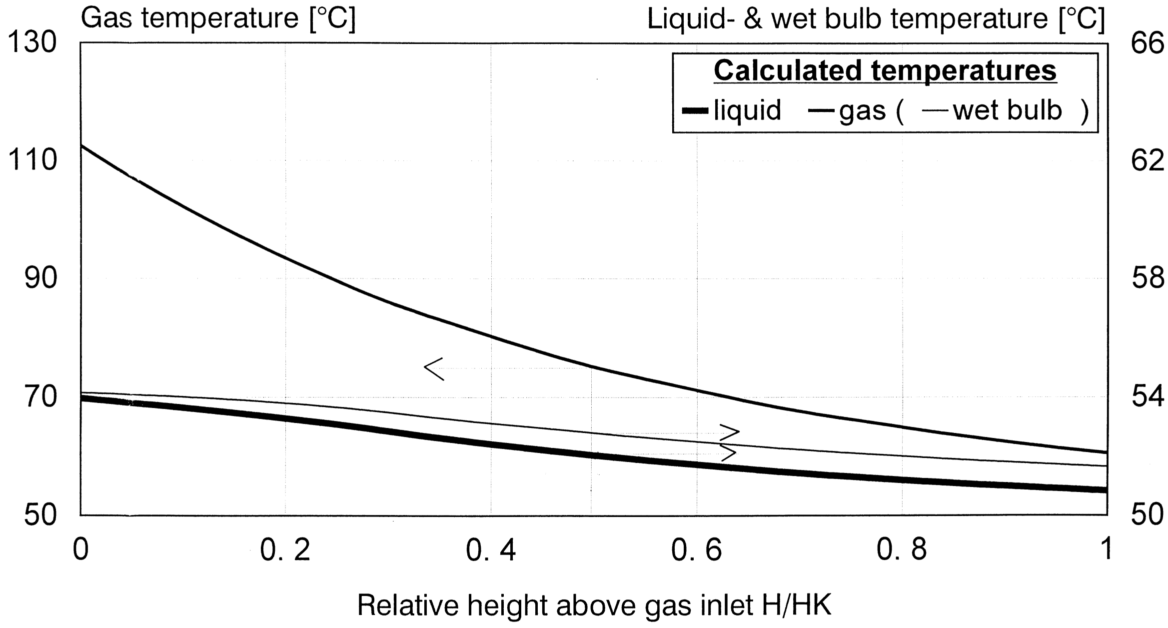

Fig. 8. Calculated temperatures for the pilot plant with closed loop.

Figs. 6 and 7 also include the wet bulb temperatures and related humidities of the gases. As it can be seen, the actual gas outlet temperature (≈48.7°C) is far away from the adiabatic saturation temperature of the inlet gases (54.1°C). Also, the actual absolute humidity at the outlet (43 g/kg) is too far from the adiabatic saturation humidity of the inlet gases (99.9 g/kg). This fact was already observed at the pilot plant and confirms the validity of the calculation.

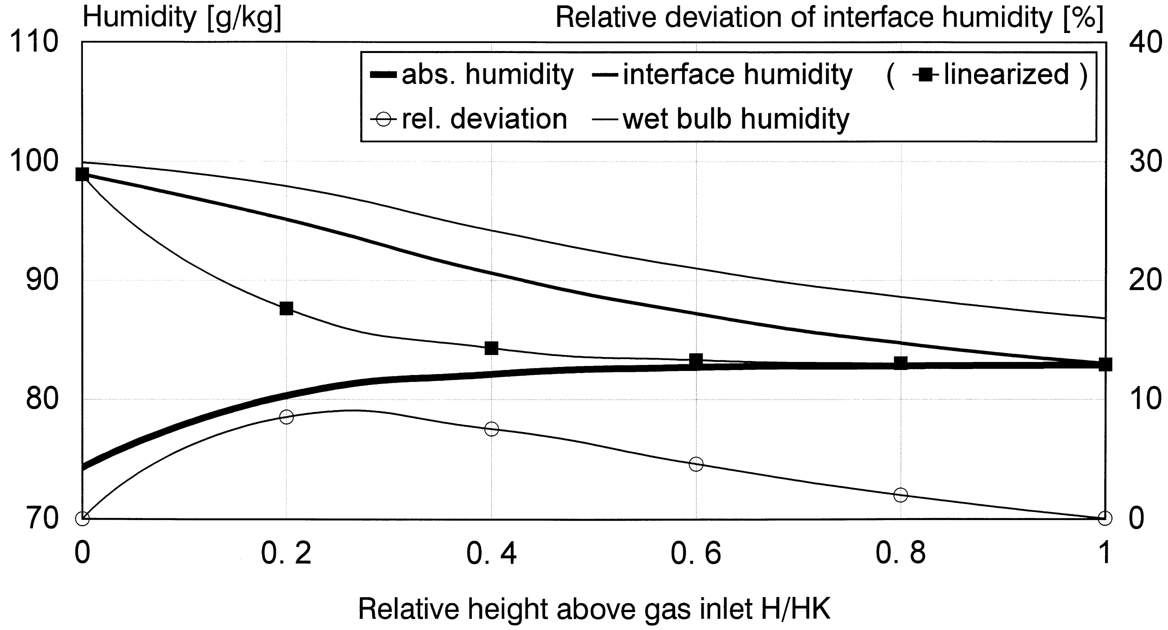

Fig. 9. Calculated humidities for the pilot plant with closed loop.

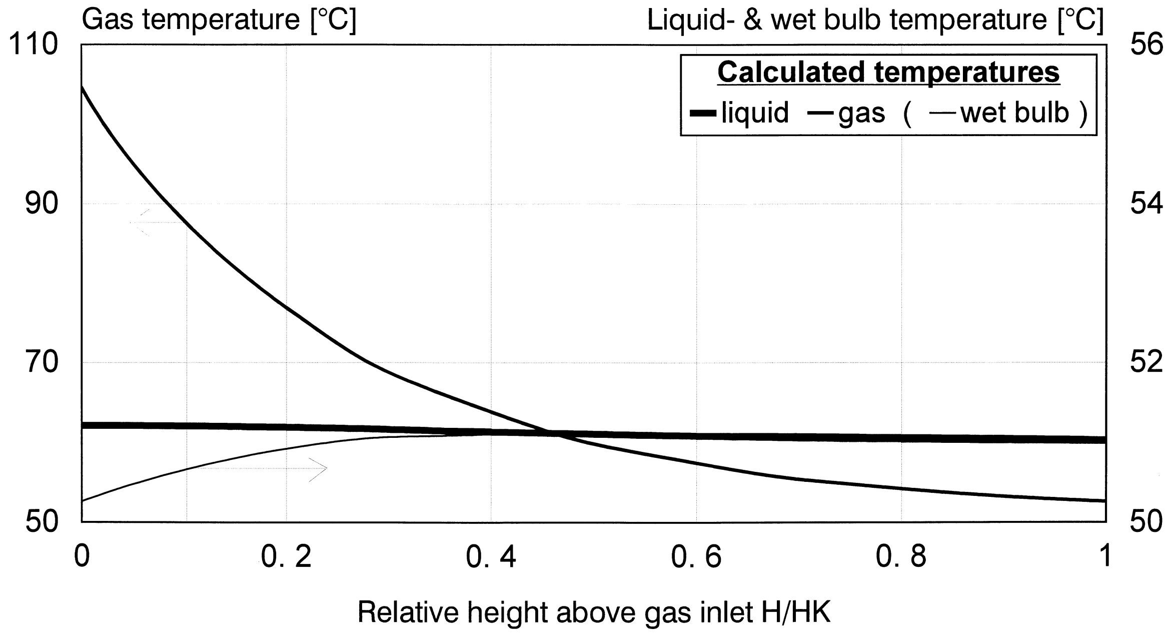

Fig. 10. Calculated temperatures in an industrial countercurrent spray absorber.

4.2. Closed loop spray tower

For a direct comparison with the open loop spray tower, the pilot plant was assumed in a first check, to operate as closed loop. Calculation results with the same Sauter diameter as found before and with an arbitrary sized effluent stream of 5 m^3/h, are shown in Figs. 8 and 9.

As it can be seen, the gas outlet temperature (≈60°C) would be increased compared to the open

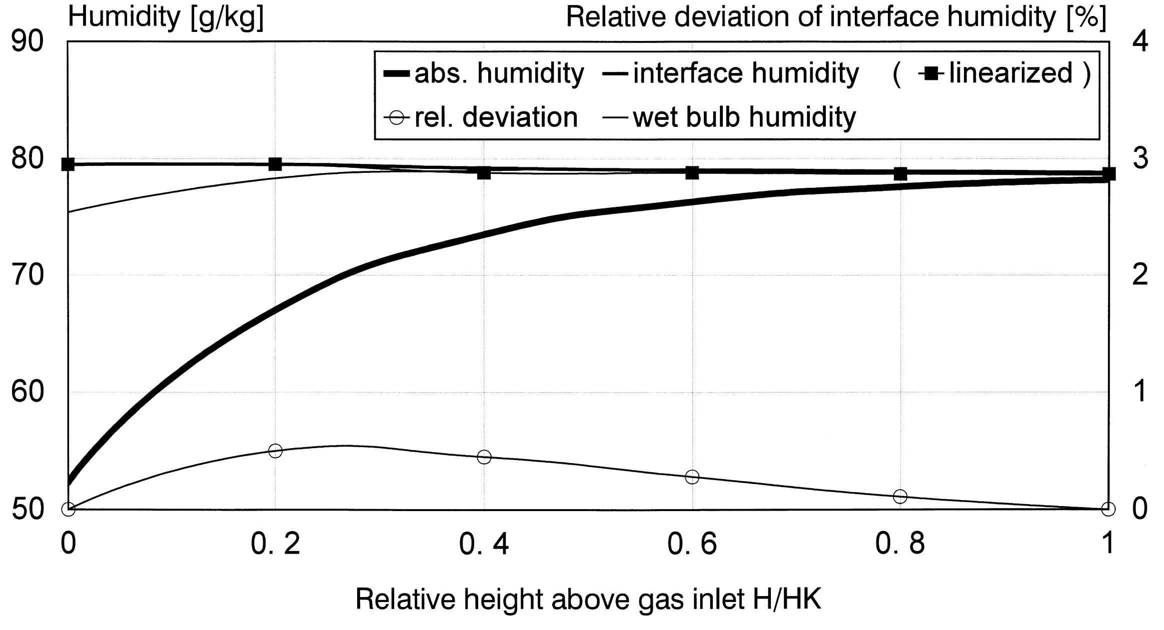

Fig. 11. Calculated humidities in an industrial countercurrent spray absorber.

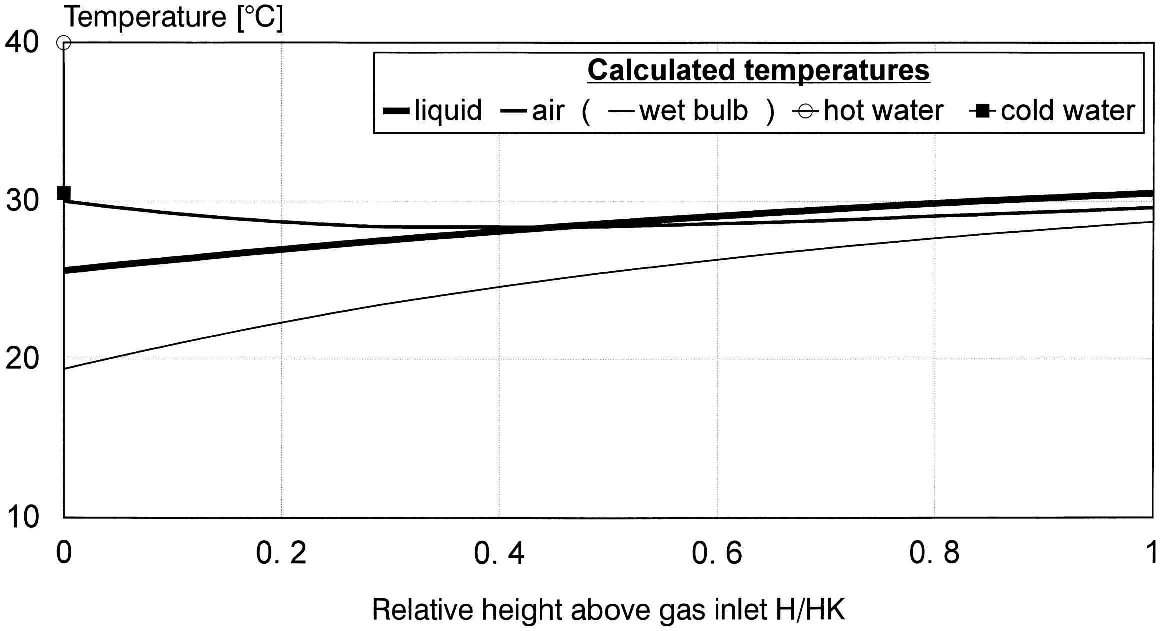

Fig. 12. Calculated temperatures in an industrial countercurrent cooling tower.

loop (48.7°C). The liquid outlet temperature (50.8°C) is now much closer to the wet bulb temperature of the inlet gases (54.1°C). However, the gas outlet temperature is still far away from this limiting temperature. This is obviously caused by the relative short contact time as well as by the small rainfall intensity of the pilot plant and the relatively large Sauter diameter in the tower.

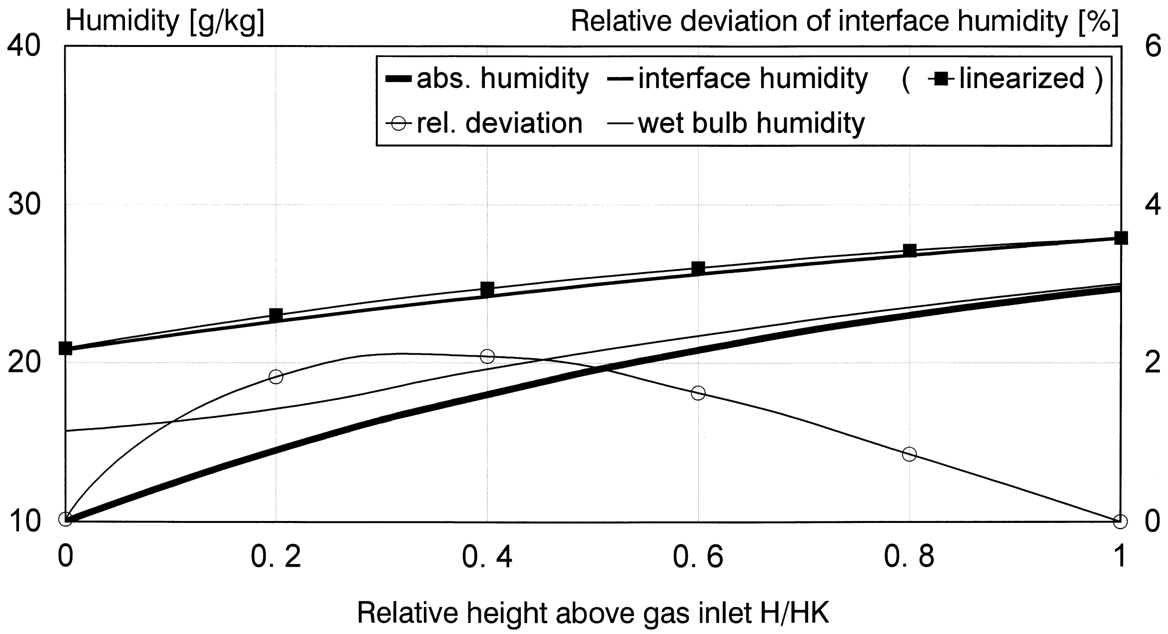

Fig. 13. Calculated humidities in an industrial countercurrent cooling tower.

For a better understanding, a second example was created and calculated. Here, the situation in a real industrial countercurrent spray tower was chosen, like those used for flue gas desulphurization with limestone as the absorbent. The tower has a diameter of 14 m and an effective contact height of 11 m, sized for a dry gas flow rate of 1,600,000 m^3/h (at 0°C and col. 3 kPa). The recycled liquid flow rate was 10,275 m^3/h. The individual nozzles have an outlet velocity of 13 m/s and generate a Sauter diameter of 2.5 mm. The Sauter diameter in the tower was assumed to be the same as for the individual nozzles. Calculation results for this tower are shown in Figs. 10 and 11.

As it can be seen, the liquid outlet temperature is very close to the wet bulb temperature of the inlet gases, but not exactly the same. The relative small deviation between the linearized and non linearized local absolute humidities at the interfaces ($<1\%$) verifies a very good suitability of the developed solution.

4.3. Closed loop liquid cooling tower

Here again, a realistic industrial case was chosen as example, a cooling tower for treatment of cooling water coming from a steel producing facility, with 6.5 m diameter and 15 m effective height. It was designed for an air flow rate of 600,000 m^3/h (at 0°C and col. 3 kPa), a hot water flow rate of 500 m^3/h and a back flow temperature of 40°C, which had to be cooled down to approximately 30°C. The make up water flow rate was 50 m^3/h with a temperature of 30°C. The chloride concentration in the system was round about 250 mg/l. The nozzles had an outlet velocity of 13 m/s, generating a Sauter diameter of 2 mm. The calculation results with this Sauter diameter are shown in Figs. 12 and 13.

The results demonstrate only small deviations ($<2.1\%$) between linearized and non linearized local absolute humidities at the interface as well; an additional proof of the suitability of the developed solutions.

References

[1] Bosnjakovic: Technische Thermodynamik, II. Teil, Dresden, 1971.

[2] Perry/Chilton, Chemical Engineers Handbook, 5th ed., New York.

[3] P.E., Harting, Zur einheitlichen Berechnung von Kühltürmen, Dissertation an der TU Braunschweig, 1977.

[4] H.-H., Brandes, Zur Berechnung der Kühlleistung und des Schwadenzustandes von Naßkühltürmen, Dissertation an der TU-Hannover, 1980.

[5] U. Häuser, Untersuchungen zum Betriebsverhalten von Hybridkühltürmen. Dissertation an der TU Braunschweig, 1981.

[6] W. Batel, Einführung in die Korngrößenmechanik, Springer-Verlag, Berlin, 1971.

[7] R. Becker, Theorie der Wärme, Springer-Verlag, Berlin, 1966.

[8] Bronstein/Semendjajew, Taschenbuch der Mathematik, 9. Auflage, Zürich, 1969.

[9] I. Szabo, Mathematik (Hütte I “Des Ingenieurs Taschenbuch”, 28. Auflage, Berlin).